

Occurrence and chemistry of xanthophyllite in roof pendants of the Bergell granite, Sondrio, Northern Italy

Autor(en): **Bucher-Nurminen, Kurt**

Objektyp: **Article**

Zeitschrift: **Schweizerische mineralogische und petrographische Mitteilungen
= Bulletin suisse de minéralogie et pétrographie**

Band (Jahr): **56 (1976)**

Heft 3

PDF erstellt am: **11.07.2024**

Persistenter Link: <https://doi.org/10.5169/seals-43693>

Nutzungsbedingungen

Die ETH-Bibliothek ist Anbieterin der digitalisierten Zeitschriften. Sie besitzt keine Urheberrechte an den Inhalten der Zeitschriften. Die Rechte liegen in der Regel bei den Herausgebern.

Die auf der Plattform e-periodica veröffentlichten Dokumente stehen für nicht-kommerzielle Zwecke in Lehre und Forschung sowie für die private Nutzung frei zur Verfügung. Einzelne Dateien oder Ausdrucke aus diesem Angebot können zusammen mit diesen Nutzungsbedingungen und den korrekten Herkunftsbezeichnungen weitergegeben werden.

Das Veröffentlichen von Bildern in Print- und Online-Publikationen ist nur mit vorheriger Genehmigung der Rechteinhaber erlaubt. Die systematische Speicherung von Teilen des elektronischen Angebots auf anderen Servern bedarf ebenfalls des schriftlichen Einverständnisses der Rechteinhaber.

Haftungsausschluss

Alle Angaben erfolgen ohne Gewähr für Vollständigkeit oder Richtigkeit. Es wird keine Haftung übernommen für Schäden durch die Verwendung von Informationen aus diesem Online-Angebot oder durch das Fehlen von Informationen. Dies gilt auch für Inhalte Dritter, die über dieses Angebot zugänglich sind.

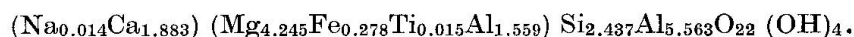
Occurrence and Chemistry of Xanthophyllite in Roof Pendants of the Bergell Granite, Sondrio, Northern Italy

By *Kurt Bucher-Nurminen* (Zürich)*)

With 2 figures, 2 plates and 6 tables

Abstract

The Ca-bearing brittle mica xanthophyllite has recently been found in the Bergell area, province Sondrio, Italy. The mineral assemblages xanthophyllite-phlogopite-forsterite-calcite and xanthophyllite-forsterite-clinohumite-spinel-calcite are found in thin, millimeters-wide bands in one of two samples studied, while xanthophyllite-diopside-phlogopite-pargasite-calcite is characteristic for an xanthophyllite-bearing band in a second sample. Under the given metamorphic conditions in the marble roof pendants in the eastern margin of the Bergell tonalite, xanthophyllite may theoretically occur in either of two different bulk compositions of aluminous marble (Al_2O_3 less than 10 wt %). These compositional requirements were met by the two samples examined. Xanthophyllite may have formed by breakdown reactions of phlogopite and/or pargasite with other silicates and/or calcite. Microprobe analysis of xanthophyllite from both rock types show little variation and yield the structural formula:



The refined lattice constants derived from powder diffraction studies are: $a = 5.20_0$, $b = 9.00_5$, $c = 9.80_0$ (in Å), $\beta = 100^\circ 18$.

1. Introduction

The mineral xanthophyllite was first described from the southern Ural mountains where it occurs in talc-chlorite-schist (ROSE, 1842). Subsequently, variously colored varieties of this mica were given individual mineralogical names, although they later were shown to be chemically and mineralogically identical (FORMAN et al., 1967). The mineral clintonite is chemically identical to xanthophyllite, but has different optical characteristics, e.g. smaller optic angle, be-

*) Institut für Kristallographie und Petrographie, ETH-Zentrum, CH-8092 Zürich, Switzerland.

lieved to be caused by polymorphism of the layer stacking (DEER, HOWIE and ZUSSMAN, 1970).

OLESCH (1975) reviewed the range of composition, solid solution and physical properties of natural clintonite and xanthophyllite. The upper thermal stability and phase relations of the clintonite-xanthophyllite solid-solution series were recently determined by OLESCH and SEIFFERT (1976). In particular, OLESCH and SEIFFERT found xanthophyllite with $Si = 1.2$ (based on 11 oxygens) to be the most stable of the solid solutions. Although the stability field of these micas was determined to be quite large, these authors explained the rarity of xanthophyllite-clintonite mica in nature as due to the restricted bulk composition requirements, and further suggested that Si-Al metasomatism was a necessary condition for formation of the mica.

Xanthophyllite has not previously been included in P-T- X_{CO_2} phase diagrams. From its geologic occurrence, however, xanthophyllite should be stable in the high-temperature, low-pressure and low- X_{CO_2} phase volumes.

A countless number of small roof pendants, or inclusions, of dolomitic marble and calc-silicate rocks can be found along the eastern margin of the Bergell granite intrusion. A large number of other silicate minerals from these metamorphic carbonate rocks has been previously described (e.g. GYR, 1967). Recently, the brittle mica xanthophyllite has been identified in several samples from impure carbonate roof pendants. The mica occurs in a similar geological setting, and is accompanied by similar minerals, as described by STRUWE (1958) from the French Pyrenees, by BIANCHI (1946) and HIEKE (1945) from Adamello, Italy, by KNOPF (1953) from the Boulder Batholith Montana, USA, and by CALLEGARI (1962) from Cima Uzza, Adamello, Italy. All of these localities are characterized by contact metamorphism of impure carbonate rocks. Xanthophyllite is typically found in magnesian carbonate rocks, close to an intrusive contact.

2. Analytical methods

Chemical analyses of the minerals were obtained using a computerized A.R.L. SEMQ electron microprobe. The analyses were carried out by routine techniques, whereby natural silicate minerals (pyroxene, olivine and feldspar) were used as standards for most silicates, and pure natural oxides were used for analyses of spinel. Data correction and reduction procedures were computed with a Fortran IV program, utilizing the 15 kV α -factors of BENCE and ALBEE. Different analyses of the same mineral listed in Table are from individual grains in that sample. For each grain, analyses of at least 10 spots were measured and finally averaged. X-ray diffraction studies were carried out on a sample of xanthophyllite from Ca 26 using powder diffraction techniques. The powder pattern was indexed using the data of FORMAN et al. (1967) and the ASTM index. Refined

Table 1. X-ray powder diffraction data of xanthophyllite of sample Ca 26

| I | h k l | d _{obs.} | d _{calc.} | I | h k l | d _{obs.} | d _{calc.} |
|-----|----------|-------------------|--------------------|----|----------|-------------------|--------------------|
| 80 | 0 0 1 | 9.61 | 9.64 | | | | |
| 7 | 0 0 2 | 4.80 | 4.82 | 20 | { -1 3 3 | 2.11 | 2.11 |
| 2 | 0 2 0 | 4.49 | 4.50 | | { 2 0 2 | 2.11 | 2.11 |
| 10 | -1 1 2 | 3.55 | 3.56 | 70 | { 0 0 5 | 1.930 | 1.929 |
| 12 | 0 2 2 | 3.29 | 3.29 | | { -1 3 4 | 1.848 | 1.850 |
| 100 | 0 0 3 | 3.23 | 3.21 | 5 | { 1 4 2 | 1.848 | 1.847 |
| 10 | 1 1 2 | 3.04 | 3.04 | | { 0 4 3 | 1.848 | 1.844 |
| 7 | -1 1 3 | 2.82 | 2.82 | | { -1 5 1 | 1.690 | 1.690 |
| 5 | 0 2 3 | 2.61 | 2.62 | 6 | { 2 4 0 | 1.690 | 1.690 |
| | | | | | { 1 3 4 | 1.690 | 1.690 |
| 25 | { -1 3 1 | 2.56 | 2.56 | | { -1 3 5 | 1.617 | 1.618 |
| | { 2 0 0 | 2.56 | 2.56 | | { -1 0 6 | 1.617 | 1.618 |
| 8 | 1 3 1 | 2.44 | 2.45 | 20 | { -3 2 1 | 1.617 | 1.618 |
| 2 | 0 0 4 | 2.41 | 2.41 | | { 2 0 4 | 1.617 | 1.616 |
| | | | | | { 0 0 6 | 1.608 | 1.607 |
| 6 | { -1 3 2 | 2.37 | 2.47 | 40 | { -3 3 1 | 1.501 | 1.501 |
| | { 2 0 1 | 2.37 | 2.37 | 16 | { -2 0 6 | 1.485 | 1.486 |
| 8 | 0 4 1 | 2.19 | 2.19 | 25 | { 1 3 5 | 1.485 | 1.484 |

Cell-dimensions (monoclinic):

a = 5.200 ± 0.002 Å, b = 9.005 ± 0.005 Å, c = 9.801 ± 0.005 Å, β = 100.30° ± 0.05°, β = 100° 18'

cell dimensions were used to calculate the possible reflections and their respective indices without regard to extinctions. A few reflections had to be reindexed, and a second refinement subsequently was carried out. For these calculations, the IDEX and X-RAY computer programs of the Institute of Crystallography of the ETH Zürich were applied.

3. Xanthophyllite-bearing marble, Bergell area

Xanthophyllite-bearing carbonate rocks are found in the Val Sissone area of the Val Malenco, Province Sondrio, northern Italy¹⁾. Aspects of the local and regional geology are given in TROMMSDORFF, PETERS and BUCHER (1975). Other occurrences have been found 200 m east of the one mentioned above, but are not discussed here.

The carbonate rocks are rather coarsegrained, with a characteristic grain size of 1–2 mm. Two representative samples were selected for analysis. Sample Ca 26 is a 2 cm thick, relatively calcite-rich calc-silicate band, interlayered with phlogopite-diopside marble. Sample Ca 25 represents a portion of a compositionally-zoned sequence of grossularite-diopside marble on one side, and olivine-spinel marble on the other.

The samples were collected from a lens- or pod-like body of xanthophyllite marble interlayered with pelitic gneiss, measuring about 50–100 m across. This

¹⁾ The coordinates referring to the Swiss coordinate network are 776.830/129.160. The locality is covered by the 1 : 25,000 map sheet 1296 (Sciora) of the Swiss Federal Topographic Service.

lens is enclosed by tonalite. No metasomatic zoning is evident in the marble at the tonalite contact, and the tonalite itself remains relatively unchanged, except for some formation epidote from hornblende and scapolite from plagioclase in an exchange zone up to several millimeters wide. The carbonate rocks are characterized throughout by alternating layers 1 to 20 cm thick of more resistant, silicate-rich bands, and by more easily weathered, carbonate-rich bands. The silicate-rich bands are often boundinaged and separated. The banding is cut discordantly by the intrusive contact. There is usually a gradual, non-symmetrical compositional variation from one band to the next, with a few millimeters or centimeters. Hence, since the carbonate rocks contain no clear evidence of large-scale metasomatic zoning the banding is therefore believed to be sedimentary in origin.

4. Conditions of metamorphism

The xanthophyllite-bearing, marble roof pendants are located about one kilometer inside the main contact of the intrusive Bergell tonalite. Pelitic rocks in nearby roof pendants contain cordierite, garnet, biotite and sillimanite (WENK et al., 1974). In some calc-silicate rocks, grossularite and quartz are present, and, because the compositionally equivalent mineral assemblage wollastonite plus anorthite has not been found, a limit of approximately 590–650° C can be placed on the temperature attained by these rocks (NEWTON, 1966; BOETTCHER, 1970; and STORRE, 1970). The isobaric, univariant assemblage wollastonite + quartz + calcite is also common. The mineral assemblage diopside + forsterite + calcite in dolomitic marbles indicates that P-T conditions were above the tremolite + calcite-out isograd of SKIPPEN (1974). Beyond the intrusive contact, andalusite occurs in pelitic rocks of relatively lower metamorphic grade. In summary these observations suggest a temperature of 600–650° C, at 2–4 kb total pressure, for the conditions of contact metamorphism.

5. Sample Ca 26

The mineral assemblage of calcite + diopside + phlogopite + olivine is characteristic for marble both above and below the xanthophyllite layer in Ca 26. The isobarically divariant, three-phase mineral assemblage calcite + diopside + forsterite can be regarded as a high-grade metamorphic product of a siliceous dolomite (SKIPPEN, 1974). Approaching the xanthophyllite layer, small isolated flakes of xanthophyllite occur first along grain boundaries of the calcite mosaic. The xanthophyllite layer, itself, contains calcite + xanthophyllite + pargasitic amphibole + diopside + phlogopite, all in mutual contact. The calcic amphibole has optical characteristics of pargasite, and microprobe analysis (Table 3) in-

Table 2. *Symbols and composition of minerals under consideration*

| Symbol | Name | Composition |
|--------|----------------|--|
| Cc | Calcite | CaCO_3 |
| Di | Diopside | $\text{CaMgSi}_2\text{O}_6$ |
| Fo | Forsterite | Mg_2SiO_4 |
| Pa | Pargasite | $\text{KCa}_2\text{Mg}_4\text{Al}_3\text{Si}_6\text{O}_{22}(\text{OH})_2$ |
| Phl | Phlogopite | $\text{KMg}_3\text{AlSi}_3\text{O}_{10}(\text{OH})_2$ |
| Xa | Xanthophyllite | $\text{Ca}_4\text{Mg}_9\text{Al}_{14}\text{Si}_5\text{O}_{40}(\text{OH})_8$ *) |
| Sp | Spinel | MgAl_2O_4 |

*) Slightly simplified stoichiometry.

Further: Do = dolomite, Hu = clinohumite, Wo = wollastonite,

Gross = grossularite.

indicated that the amphiboles contain more than 90 mole-% end-member pargasite. Two pargasite generations may be distinguished, one of which is somewhat larger in grain size, with slightly embayed grain boundaries. Both pargasites are pleochroitic and have a positive optical character. There is no apparent compositional difference between the two generations of amphibole. Diopside pyroxene forms small, rounded grains. Xanthophyllite forms fresh, euhedral grains with a pleochroism from colorless along α , to pale brown along γ . Undeformed, large crystals exhibit perfect cleavage parallel (001). In the xanthophyllite layer, the brittle mica is most commonly associated with pargasite and diopside. The textures do not suggest any particular xanthophyllite-forming reaction, and the phases are commonly in textural equilibrium (mosaic texture). The microtexture of this rock shows little deformation, grain boundaries are sharp and straight, although the phlogopite-rich mica is occasionally kinked.

6. Sample Ca 25

An interesting and somewhat different occurrence of xanthophyllite was found in a sequence of compositionally zoned carbonate rocks. This rock-type has a banded appearance, with a calc-silicate band on one side, siliceous dolomite band on the other and a band of variable, intermediate composition between these two bands. The change in composition in the sample takes place over a distance of 2–3 cm. The characteristics of the mineralogical zones are described in detail below, and the chemical composition of several minerals from the zones are listed in Table 3 and Table 4 respectively.

Zone 1: Clinohumite + olivine + spinel + calcite. Colorless clinohumite is often twinned, rather coarse-grained, and commonly shows resorption features. Olivine forms relatively smaller fresh, rounded grains. Green spinel, which frequently contains inclusions of magnetite and ilmenite, coexists with small, yellow-brown grains of perovskite. The most abundant mineral in this zone is undeformed, coarse-grained Mg-calcite.

Table 3. *Microprobe analyses of xanthophyllite, phlogopite and pargasite*

| | Xanthophyllite | | | | | | Phlogopite | | Pargasite | |
|------------------------------------|----------------|---------|---------|---------|---------|---------|------------|-------|-----------|---------|
| | Ca 25 A | Ca 25 B | Ca 25 C | Ca 26 A | Ca 26 B | Ca 26 C | Ca 25 | Ca 26 | Ca 26 A | Ca 26 B |
| SiO ₂ | 17.47 | 16.88 | 17.05 | 16.32 | 17.43 | 17.29 | 38.90 | 38.48 | 40.03 | 39.88 |
| TiO ₂ | 0.14 | 0.19 | 0.18 | 0.13 | 0.10 | 0.09 | 0.40 | 0.24 | 0.50 | 0.37 |
| Al ₂ O ₃ | 43.22 | 43.47 | 43.09 | 46.14 | 43.89 | 44.22 | 17.55 | 19.82 | 18.40 | 18.91 |
| Fe as FeO | 2.38 | 2.39 | 2.44 | 2.39 | 2.47 | 2.50 | 1.74 | 2.80 | 5.68 | 5.64 |
| MnO | 0.00 | 0.00 | 0.00 | 0.00 | 0.00 | 0.00 | 0.00 | 0.00 | 0.11 | 0.00 |
| MgO | 20.37 | 19.81 | 19.97 | 19.15 | 19.80 | 19.66 | 25.36 | 24.60 | 16.55 | 16.02 |
| CaO | 12.57 | 12.75 | 12.40 | 12.16 | 12.06 | 12.55 | 0.00 | 0.06 | 12.84 | 12.87 |
| Na ₂ O | 0.05 | 0.04 | 0.04 | 0.12 | 0.27 | 0.21 | 0.06 | 0.32 | 2.07 | 1.98 |
| K ₂ O | 0.00 | 0.00 | 0.00 | 0.00 | 0.00 | 0.00 | 11.20 | 10.11 | 2.07 | 2.27 |
| Total | 96.15 | 95.53 | 95.17 | 96.41 | 96.03 | 96.22 | 95.21 | 96.43 | 98.25 | 97.94 |
| Atoms*) per formula unit | | | | | | | | | | |
| Si | 2.437 | 2.379 | 2.409 | 2.271 | 2.437 | 2.413 | 5.490 | 5.351 | 5.757 | 5.751 |
| Al ^{IV} | 5.563 | 5.621 | 5.591 | 5.729 | 5.563 | 5.587 | 2.510 | 2.649 | 2.243 | 2.249 |
| Al ^{VI} | 1.559 | 1.599 | 1.585 | 1.838 | 1.668 | 1.688 | 0.419 | 0.600 | 0.876 | 0.965 |
| Ti | 0.015 | 0.020 | 0.019 | 0.014 | 0.011 | 0.009 | 0.042 | 0.025 | 0.054 | 0.040 |
| Fe**) Fe^{2+} | 0.278 | 0.282 | 0.288 | 0.278 | 0.289 | 0.292 | 0.205 | 0.326 | 0.683 | 0.680 |
| Mn | 0.000 | 0.000 | 0.000 | 0.000 | 0.000 | 0.000 | 0.000 | 0.000 | 0.013 | 0.000 |
| Mg | 4.245 | 4.161 | 4.201 | 3.970 | 4.126 | 4.090 | 5.335 | 5.099 | 3.547 | 3.443 |
| $\sum \text{Al}^{\text{VI to Mg}}$ | 6.097 | 6.062 | 6.098 | 6.100 | 6.094 | 6.079 | 6.001 | 6.050 | 5.173 | 5.128 |
| Ca | 1.883 | 1.925 | 1.877 | 1.813 | 1.806 | 1.832 | 0.000 | 0.009 | 1.978 | 1.988 |
| Na | 0.014 | 0.011 | 0.014 | 0.032 | 0.073 | 0.057 | 0.016 | 0.086 | 0.577 | 0.554 |
| K | 0.000 | 0.000 | 0.000 | 0.000 | 0.000 | 0.000 | 2.016 | 1.794 | 0.380 | 0.418 |
| $\sum \text{Ca to K}$ | 1.897 | 1.936 | 1.891 | 1.845 | 1.879 | 1.889 | 2.032 | 1.889 | 2.935 | 2.960 |

*) Normalized to 22 oxygens for xanthophyllite and phlogopite, and to 23 oxygens for pargasite.

**) $\text{Fe}_{\text{total}} = \text{Fe}^{2+}$.

Fluorine in all hydrous minerals was below detectable limit ($< 0.1\% \text{F}_2$).

Table 4. *Microprobe analyses of olivine, diopside and spinel of sample Ca 25*

| Weight% oxides | Olivine | Pyroxene | Spinel |
|--------------------------------|---------|----------|--------|
| SiO ₂ | 42.01 | 53.52 | 0.12 |
| TiO ₂ | 0.02 | 0.23 | 0.05 |
| Al ₂ O ₃ | — | 0.89 | 68.20 |
| Fe as FeO | 2.53 | 1.17 | 7.00 |
| MnO | 0.16 | 0.05 | 0.06 |
| MgO | 54.72 | 16.67 | 24.31 |
| CaO | 0.13 | 27.12 | 0.03 |
| Na ₂ O | — | 0.02 | — |
| K ₂ O | — | — | — |
| Total | 99.55 | 99.67 | 99.77 |

Structural formulas:

Olivine (based on 4 ox.) $(\text{Ca}_{0.003}\text{Mn}_{0.003}\text{Mg}_{1.942}\text{Fe}_{0.05}\text{Ti}_{0.001})_{1.999}[\text{Si}_{1.0}]_4\text{O}_4$

Pyroxene (based on 6 ox.) $(\text{Ca}_{1.064}\text{Mn}_{0.002}\text{Mg}_{0.91}\text{Fe}_{0.036}\text{Ti}_{0.006})_{2.019}[\text{Si}_{1.959}\text{Al}_{0.038}]_{1.997}\text{O}_6$

Spinel (based on 32 ox.) $(\text{Mn}_{0.008}\text{Fe}_{1.152}\text{Mg}_{7.112})_{8.272}[\text{Ti}_{0.00}\text{Si}_{0.024}\text{Al}_{15.776}]_{15.808}\text{O}_{32}$

Transition zone 1a: Xanthophyllite + olivine + clinohumite + spinel + calcite. In this zone, xanthophyllite with brownish birefringence occurs in contact with minerals of zone 1.

Zone 2: Xanthophyllite + calcite + phlogopite + olivine. The grain size of calcite in this 5–10 mm wide zone is finer than in other zones. Euhedral, undeformed xanthophyllite crystals show reddish-brown to reddish-blue birefringence, and have a $2V$ of zero to five degrees. Xanthophyllite is the characteristic mineral of zone 2, and constitutes about 10% of the mineral assemblage (Plate 1). Pale-colored phlogopite is intergrown with xanthophyllite.

Transition zone 2a: Xanthophyllite + calcite + phlogopite + olivine. This zone is characterized by the disappearance of xanthophyllite. Parallel intergrowths of xanthophyllite and phlogopite are typical (Plate 2), but are found only over a very small region (~ 2 mm).

Zone 3: Phlogopite + olivine + calcite. The width of zone 3 is about 10 mm. Phlogopite is finer-grained and less abundant than in zone 3.

Transition zone 3a: Phlogopite + olivine + diopside + calcite. Phlogopite and olivine disappear within this transition zone, while diopside makes its first appearance in the form of small euhedral crystals.

Zone 4: Diopside + calcite + grossularite. Diopside and calcite are the most

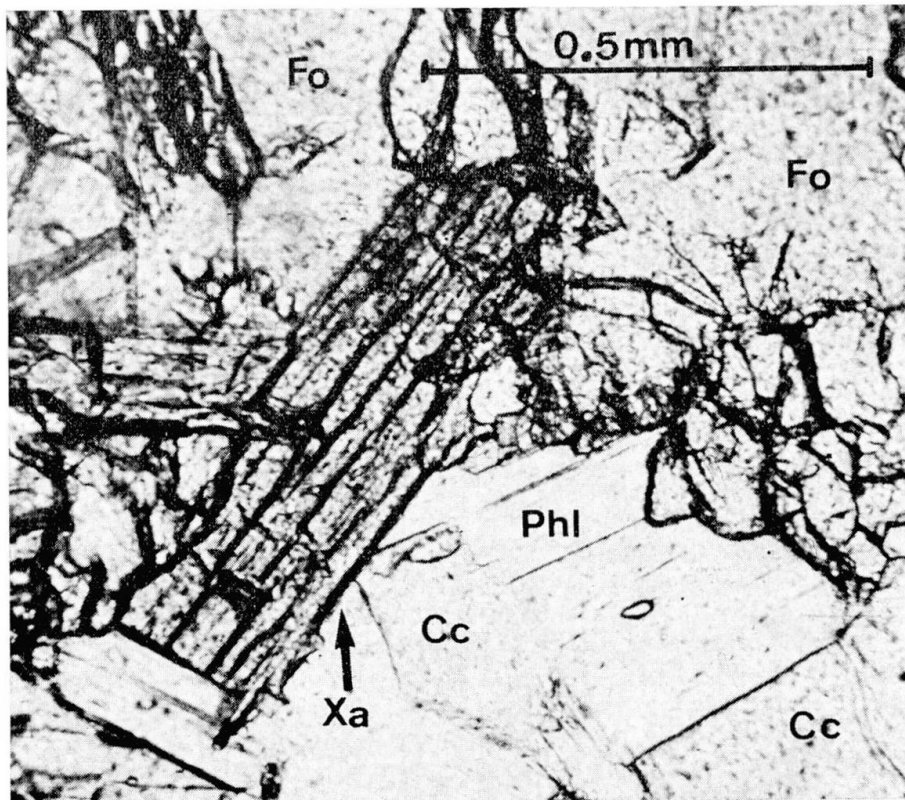


Plate 1. Photomicrograph of xanthophyllite bearing assemblage of sample Ca 25 (Zone 2). Parallel polarizers.

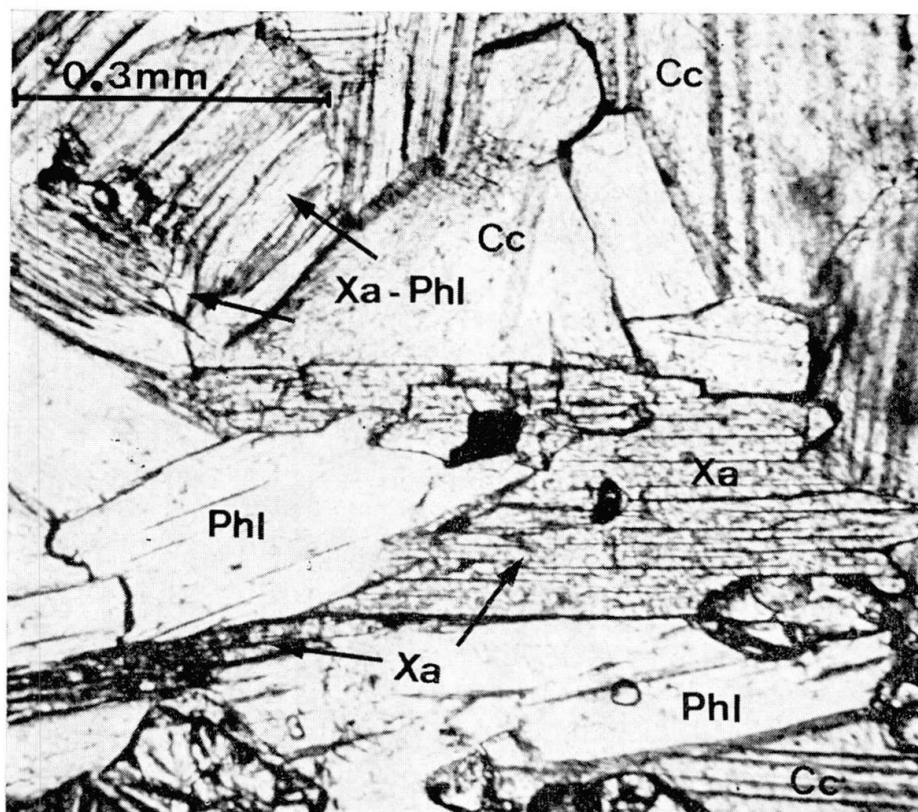


Plate 2. Photomicrograph of xanthophyllite assemblage of sample Ca 25 (Zone 2a). Note xanthophyllite-phlogopite intergrowth. Parallel polarizers.

abundant constituents of zone 4. Coarse-grained grossularite contains inclusions of diopside and calcite, but exhibits embayed grain boundaries.

Apart from the xanthophyllite-phlogopite intergrowth, which suggests replacement of phlogopite by xanthophyllite in zone 2a (Plate 2), no reaction textures were observed. It is noteworthy that xanthophyllite is restricted to phlogopite-bearing zones, and that microtextures suggest the formation of xanthophyllite at the expense of phlogopite.

Table 5. Observed mineral assemblages among minerals of Table 2 involving xanthophyllite

| Assemblage | *) | Locality, Reference |
|-------------------------|--------|--|
| Xa - Cc - Di - Phl - Pa | Fo Sp | Bergell Ca 26 |
| Xa - Cc - Fo - Phl - Sp | Di Pa | Bergell Ca 25 |
| Xa - Cc - Di - Fo - Sp | Phl Pa | various localities (OLESCH et al., 1976) |
| Xa - Cc - Di - Fo - Phl | Pa Sp | Adamello (BUCHER, unpub. data) |
| Xa - Cc - Di - Sp - Phl | Pa Fo | Adamello (CALLEGARI, 1962) |

*) Notation with absent minerals not present in the assemblage.

7. Discussion: Formation of xanthophyllite

Phlogopite, chlorite and pargasitic amphibole in Al-bearing siliceous dolomite react with carbonates and/or silicates at relatively high metamorphic grades to produce spinel (GLASSLEY, 1975; BUCHER, 1976).

Under certain conditions, the Al-bearing breakdown product is not anhydrous spinel, but rather xanthophyllite, containing normally about 44% Al_2O_3 (see Table 3). The occurrence of xanthophyllite in marbles in contact metamorphic terrains within meters of the intrusive contact suggests that xanthophyllite plus calcite are stable together under relatively low-pressure, low- X_{CO_2} conditions. From chemographic relations, a list of possible breakdown reactions for phlogopite and pargasite is presented in Table 6.

The amphibole occurring in metamorphosed siliceous dolomites tends to become pargasitic in the presence of Al-bearing minerals such as phlogopite, chlorite or spinel, and may closely approach the composition of the pargasite end-member in high-grade marble (GLASSLEY, 1975; BUCHER, unpubl. data). As a consequence, xanthophyllite can be expected to be a reaction product of a breakdown reaction of pargasite and/or sheet silicate such as chlorite or phlogopite.

Figure 1 shows the compositions of coexisting minerals in the samples studied, projected from K_2O onto the anhydrous $\text{SiO}_2\text{-MgO}-\frac{1}{2}\text{Al}_2\text{O}_3$ plane. Calcite and a

Table 6. Stoichiometric coefficients of reaction equations

| | 1 | 2 | 3 | 4 | 5 | 6 | 7 | 8 | 9 | 10 | |
|----------------------|-------|-------|-------|--------|--------|--------|--------|--------|-------|--------|-------|
| *) | Fo Sp | Fo Pa | Fo Xa | Fo Phl | Fo Cc | Fo Di | Di Sp | Di Pa | Di Xa | Di Phl | |
| Calcite | -56 | -3 | -7 | -5 | - | -34 | -78 | -28 | -14 | -44 | |
| Diopside | 86 | -13 | 15 | 1 | 34 | - | - | - | - | - | |
| Forsterite | - | - | - | - | - | - | 86 | 13 | 15 | 1 | |
| Phlogopite | -11 | 2 | -2 | - | -5 | 1 | -109 | -16 | -19 | - | |
| Xanthophyllite | 7 | 4 | - | 2 | -7 | 15 | -1 | 7 | - | 19 | |
| Spinel | - | -29 | 7 | -11 | 56 | -86 | - | -41 | -1 | -109 | |
| Pargasite | -29 | - | -4 | -2 | -3 | -13 | 41 | - | 7 | -16 | |
| CO_2 | 56 | 3 | 7 | 5 | - | 34 | 78 | 28 | 14 | 44 | |
| H_2O | 12 | -18 | 6 | -6 | 36 | -48 | 72 | -12 | 12 | -60 | |
| $\text{KO}_{1/2}$ | 40 | -2 | 6 | 2 | 8 | 12 | 68 | 16 | 12 | 16 | |
| *) | 11 | 12 | 13 | 14 | 15 | 16 | 17 | 18 | 19 | 20 | 21 |
| | Di Cc | Cc Sp | Cc Pa | Cc Xa | Cc Phl | Phl Sp | Phl Pa | Phl Xa | Xa Sp | Xa Pa | Pa Sp |
| Calcite | - | - | - | - | - | -61 | -8 | -7 | -7 | -7 | -53 |
| Diopside | - | -78 | 28 | -2 | 44 | 109 | -16 | 19 | 1 | 7 | 41 |
| Forsterite | 34 | 56 | 3 | 1 | -5 | -11 | 2 | -2 | 7 | 4 | 29 |
| Phlogopite | -44 | -61 | -8 | -1 | - | - | - | - | -9 | -6 | -42 |
| Xanthophyllite | -14 | -7 | -7 | - | -7 | 9 | 6 | - | - | - | 3 |
| Spinel | 78 | - | 53 | -1 | 61 | - | -42 | 9 | - | 3 | - |
| Pargasite | 28 | 53 | - | 1 | -8 | -42 | - | -6 | 3 | - | - |
| CO_2 | - | - | - | - | - | 61 | 8 | 7 | 7 | 7 | 53 |
| H_2O | 72 | 36 | 36 | - | 36 | 6 | -24 | 6 | 6 | 6 | 30 |
| $\text{KO}_{1/2}$ | 16 | 8 | 8 | - | 8 | 42 | - | 6 | 6 | 6 | 42 |

*) Notation with phases not participating in the reaction (absent phases).

C-O-H fluid phase are assumed to be present in excess. This representation implies that the fluid also contains potassium.

The mineral assemblages of sample Ca 26 can be explained by reactions occurring within bulk compositions varying along the fields schematically plotted in Figure 1. Diopside, phlogopite, forsterite and calcite are found adjacent to both sides of the xanthophyllite zone, in a bulk composition low in SiO_2 , but enriched in MgO, relative to the mineral assemblage xanthophyllite + phlogopite + pargasite + diopside + calcite of the central xanthophyllite zone. Xanthophyllite in sample Ca 26 appears to have formed by reaction 1 (Table 6), which is represented in Figure 1 by the broken tieline between pargasite and phlogopite. The fact that pargasite and phlogopite are both present with xanthophyllite and diopside merely indicates that reaction did not proceed to completion.

The formation of xanthophyllite in sample Ca 25 is more problematic. The variation in composition of the zones in Ca 25 is similar to that in Ca 26. The bulk compositions of the numbered zones described above are plotted in Figure 1. In the low SiO_2 , high MgO part of the sample, divariant, four-phase mineral assemblages are present. However, when the bulk composition of the rock crosses the forsterite-phlogopite tieline, i.e. in progressing from zone 2 to zone 3, the number of minerals is reduced by one. This indicates that the chemical potential of one chemical species becomes externally controlled approaching the grossularite + diopside + calcite band (zone 4). If, in a phlogopite-bearing

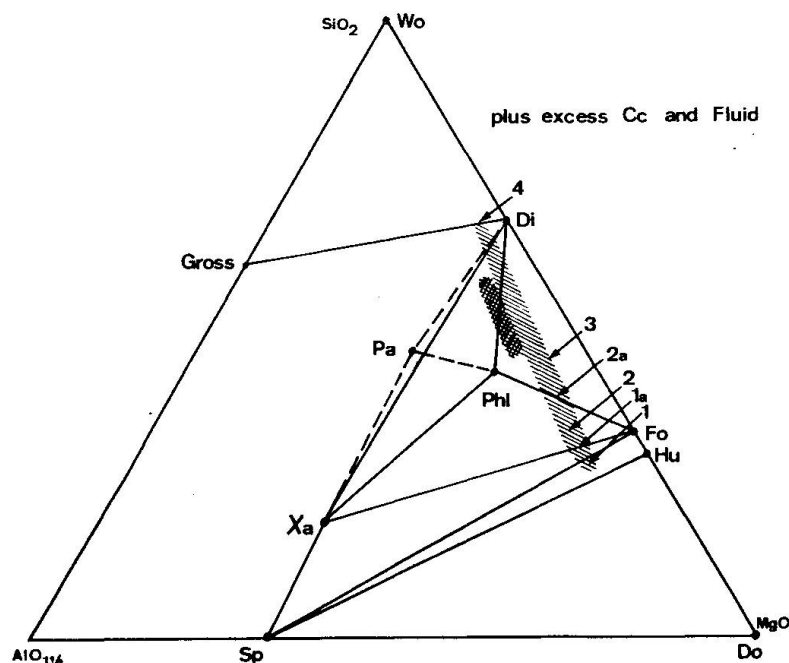


Fig. 1. Solid phase composition relations in the triangle $\text{MgO-SiO}_2\text{-AlO}_{1.5}$. Calcite and a $\text{CO}_2\text{-H}_2\text{O-KO}_{1/2}$ fluid are present in excess. Dashed area represents the compositional range of sample Ca 25 (zone numbers \rightarrow see text). Heavy dashed field shows the compositional range of sample Ca 26.

dolomite layer, all the chemical potentials were defined by the adjacent mineral assemblages of dolomite + calcite + forsterite (clinohumite) + spinel on one side, and by wollastonite + grossularite + diopside + calcite on the other, two xanthophyllite zones could be expected to develop between the buffering mineral assemblages (see Figure 1). Xanthophyllite in sample Ca 25 occurs in one of these two possible compositional regions only, and may have formed according to reaction 8 given in Table 6.

The mineral assemblages which formed in samples Ca 25 and Ca 26 are functions of composition, among other variables. The origin of the variation in bulk composition of these samples is therefore of interest. Two basic models are apparent. An "isochemical" model, whereby the variation in composition of the layering is due to the interlayering of several different sedimentary layers.

In the second model, the initial chemical composition of the sedimentary rock is assumed to have been simpler, and that local differential movement of chemical elements occurred during metamorphism in response to chemical potential or pressure gradients. The increase in variance of the mineral assemblages across zones noted above in sample Ca 25, however, supports at least some migration of elements. The textural relations of phlogopite are the only ones observed that clearly indicate the relative instability of any of the minerals. Phlogopite is clearly the most important mineral with respect to the formation of xanthophyllite, as indicated, for example, by the parallel intergrowth of both minerals.

Excluding spinel in one layer of sample Ca 25, phlogopite represents the only aluminium-bearing mineral in zones adjacent to xanthophyllite layers of both samples. Therefore, phlogopite is most likely the principal Al-source for the formation of xanthophyllite. Phlogopite and pargasite²⁾ are the only potassium-bearing minerals in both rocks. Hence, reactions involving these minerals will consume or release potassium, which is assumed to be dissolved as potassium ion and complexes in the metamorphic fluid. The stability of phlogopite in the rocks described may therefore be a function of $\mu_{\text{KO}_{1/2}}$ in addition to the composition of the C-O-H fluid, temperature and pressure. Figure 2 shows the relative stabilities of the minerals calcite, xanthophyllite, diopside, forsterite, phlogopite, pargasite and spinel in terms of μ_{CO_2} and $\mu_{\text{KO}_{1/2}}$. The stoichiometric coefficients of the reactions considered are given in Table 6. In principle, two topologies in this μ - μ diagram are possible. The invariant assemblages with [Cc], [Xa], [Pa] and [Fo] absent constitute one topology (shown in Figure 2). Alternatively, a topology including the invariant assemblages with [Di], [Sp] and [Phl] absent could also be drawn. No decision can be made at present as to which one of those

²⁾ Pargasite of sample Ca 26 contains a considerable amount of potassium (see Table 3). Pargasite is therefore treated as pure K-pargasite in the subsequent discussion. Neglecting the Na-content of the amphibole does not alter the conclusions.

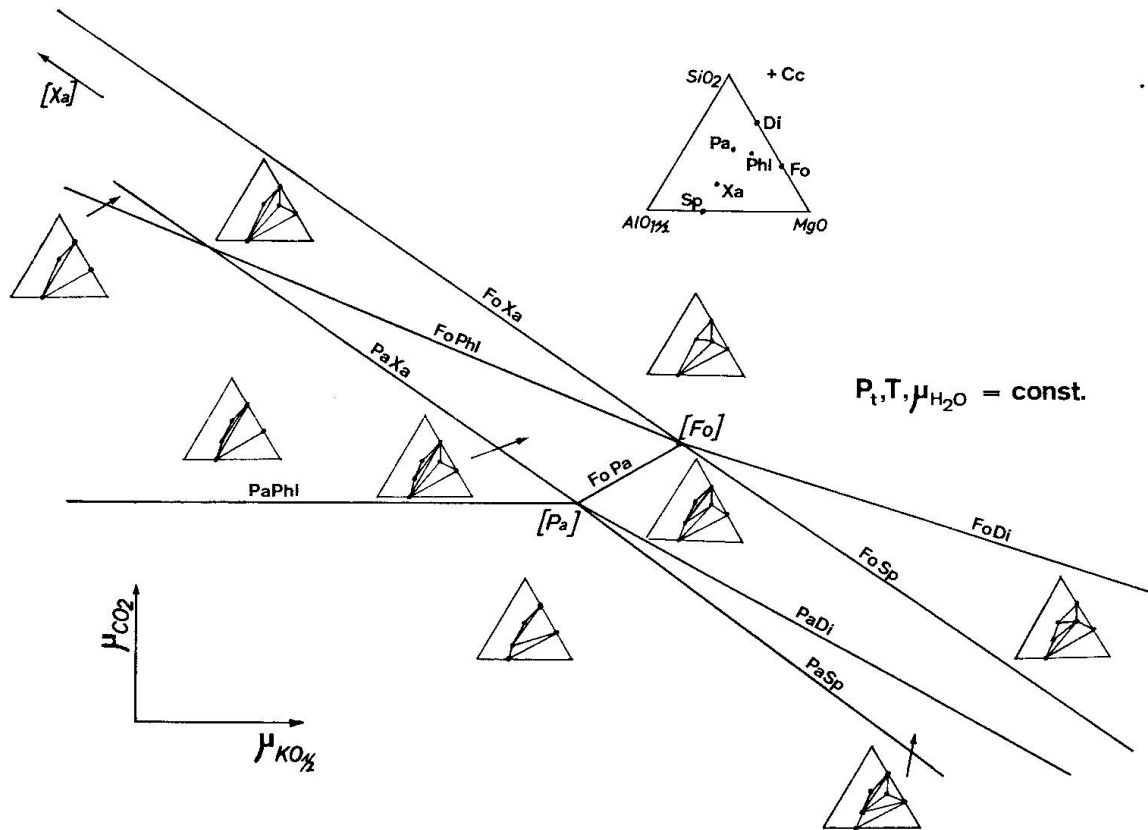


Fig. 2. μ_{CO_2} - $\mu_{\text{KO}_{1/2}}$ chemical potential diagram for reactions tabulated in Table 6. Reactions are labeled with phases not participating in the reaction (absent phases). The diagram represents the topology with Xa, Pa and Fo absent invariant points.

topologies is more stable at a given pressure and temperature, although the assemblage with Fo and Pa absent of Table 5 suggests that the topology of Figure 2 can be stable. The following conclusions are not, however, affected by the choice of the topology.

From Figure 2, it is apparent that the formation of xanthophyllite in calcite marbles requires either rather special bulk compositions of the rocks (OLESCH and SEIFFERT, 1976), or low, possibly very-low μ_{CO_2} conditions. The stability field of the four-phase mineral assemblage Xa + Di + Fo + Cc (OLESCH et al., 1976, this work) can be attributed to a decrease in μ_{CO_2} under either low $\mu_{\text{KO}_{1/2}}$ or high $\mu_{\text{KO}_{1/2}}$ conditions. In the first case, the formation of xanthophyllite occurs mainly in response to the stability limit of Cc + Di + Sp³), in a presumably very water-rich fluid. The second case leads to a number of xanthophyllite + phlogopite-bearing assemblages, as is observed in the Bergell samples and rocks from

³) Mg-spinel is thought to have been formed by breakdown reactions involving chlorite + carbonate minerals. Mg-spinel is a very frequent constituent of aluminous-siliceous dolomite marble, and the assemblage calcite + forsterite + diopside + spinel is commonly observed in these rocks (BUCHER, 1976).

the Adamello area (CALLEGARI, 1962). The four-phase mineral region $Xa + Di + Fo + Cc$ is bounded by the breakdown of phlogopite + calcite (Table 6). In general, the formation of xanthophyllite requires low μ_{CO_2} and $\mu_{K_{O1/2}}$ conditions. High $\mu_{K_{O1/2}}$ stabilizes phlogopite relative to xanthophyllite. Low μ_{CO_2} conditions in the Bergell roof-pendants are indicated by brucite-bearing, dolomitic marble bands in the calc-silicate marbles.

The typically restricted occurrence of xanthophyllite to impure carbonates in close contact to intrusive rocks suggests the dilution of an initially CO_2 -richer fluid (due to decarbonation reactions in the course of metamorphism) with magmatic water (compare TAYLOR, 1976). In addition, this water, if derived from quartz-diorite, tonalite or gabbro, might be relatively low in potassium, i.e. low $\mu_{K_{O1/2}}$.

Acknowledgments

I would like to express my sincere thanks to Bruce Taylor for critically reading the manuscript and suggesting valuable alterations. Support of Schweizerischer Nationalfonds, No. 2.249-0.74, is gratefully acknowledged.

References

- BIANCHI, A. e O. HIEKE (1946): La xanthophyllite dell'Adamello meridionale. *Periodico di Mineralogia*, anno XV, 87-134.
- BOETTCHER, A. L. (1970): The system $CaO-Al_2O_3-SiO_2-H_2O$ at high pressure and temperatures. *Jour. Petrol.* 11, 337.
- BUCHER-NURMINEN, K. (1976): Chlorit-Spinell-Paragenesen aus Dolomitmarmoren des Bergell-Ostrandes. *Schweiz. Mineral. Petrogr. Mitt.* 56, 95-100.
- CALLEGARI, E. (1962): La cima Uzza (parte I). *Mem. Ist. Geol. Miner. Univ. Padova*, volume XXIII.
- DEER, W. A., R. A. HOWIE and J. ZUSSMAN (1970): *An Introduction to the Rock Forming Minerals*. London, Longmans, Green and Co., Ltd.
- FORMAN, S. A., H. KODAMA and S. ABBEY (1967): A re-examination of xanthophyllite (clintonite) from type locality. *Can. Mineralogist* 9, 25-30.
- GLASSLEY, W. E. (1975): High grade regional metamorphism of some carbonate bodies: Significance for the orthopyroxene isograd. *Amer. J. Sci.* 275, 1133-1163.
- GYR, TH. (1967): Geologische und petrografische Untersuchungen am Ostrande des Bergeller Massivs. *Mitt. Geol. Inst. ETH und Univ. Zürich*, N. F. 66.
- HIEKE, O. (1945): I giacimenti di contatto del M. Costone (Adamello meridionale). *Mem. Ist. Geol. Univ. Padova*, vol. XV, 1-44.
- KNOFF, A. (1953): Clintonite as a contact-metasomatic product of the Boulder batholith, Montana. *Amer. Miner.* 39, 1113-1117.
- NEWTON, R. C. (1966): Some calc-silicate equilibrium relations. *Am. J. Sci.* 264, p. 204.
- OLESCH, M. (1975): Synthesis and solid solubility of trioctahedral brittle micas in the system $CaO-MgO-Al_2O_3-SiO_2-H_2O$. *Am. Miner.* 60, 188-199.
- OLESCH, M. and F. SEIFFERT (1976): Stability and phase relations of trioctahedral calcium brittle micas (clintonite group). *J. Petrol.* 17, 291-314.
- ROSE, G. (1842): *Reise nach dem Ural*, 2. Berlin.

- SKIPPEN, G. (1974): An experimental model for low pressure metamorphism of silicious dolomitic marble. *Am. J. Sci.*, Vol. 274.
- STORRE, B. (1970): Stabilitätsbedingungen Grossular-führender Paragenesen im System $\text{CaO-Al}_2\text{O}_3\text{-SiO}_2\text{-CO}_2\text{-H}_2\text{O}$. *Contr. Mineral. and Petrol.* 29, 145-162.
- STRUWE, H. (1958): Data on the mineralogy and petrology of the dolomite-bearing northern contact zone of the Quérigut granite, French Pyrenees. *Leid. geol. Med.* 22, 235-349.
- TAYLOR, B. E. (1976): Origin and significance of C-O-H fluids in the formation of Ca-Fe-Si skarn, Osgood Mountains, Humboldt County, Nevada. Unpublished Ph. D dissertation, Stanford University, Calif.
- TROMMSDORFF, V., T. J. PETERS and K. BUCHER (1975): Exkursion Bernina-Malenco-Bergell Ostrand. *Schweiz. Mineral. Petrogr. Mitt.* 55, 590-600.
- WENK, H. R., E. WENK and J. H. WALLACE (1974): Metamorphic mineral assemblages in pelitic rocks of the Bergell Alps. *Schweiz. Mineral. Petrogr. Mitt.* 54, 507-554.

Manuscript received September 21, 1976.